

Cyclin-dependent kinase like 3 promotes triple-negative breast cancer progression via inhibiting the p53 signaling pathway

Dong-Xiang ZENG¹, Gui-Feng SHENG¹, Yong-Ping LIU¹, Ya-Ping ZHANG¹, Zheng QIAN², Zhe LI^{2*}, Yan-Zhi BI^{1*}

¹Department of Medical Oncology, Changzhou Tumor Hospital Affiliated to Soochow University, Changzhou, China; ²Department of Breast Surgery, Shanghai Shuguang Hospital Affiliated to Shanghai University of Traditional Chinese Medicine, Shanghai, China

*Correspondence: biyanzhi222@163.com; lizhezsh@shutcm.edu.cn

Received March 31, 2021 / Accepted May 17, 2021

It has been reported that cyclin-dependent kinase like 3 (CDKL3) plays a crucial role in cell proliferation and migration in several cancers. However, the function of CDKL3 in triple-negative breast cancer (TNBC) is still unclear. In the present study, immunohistochemistry (IHC) was conducted to detect the CDKL3 expression. CCK-8, flow cytometry, Transwell assays, and mice xenograft models, were performed to explore the roles of CDKL3 on the proliferation and migration of TNBC *in vitro* and *in vivo*. Besides, protein chip analysis was used to screen the potential pathways, which was further confirmed by promoter activity assay, western blotting, and CCK-8 assay. Our findings reveal a high expression of CDKL3 in TNBC tissues, which is closely related to a poor prognosis of patients with TNBC. In TNBC cells, CDKL3 knockdown inhibits cell proliferation and migration, whereas CDKL3 overexpression has exactly the opposite effect. Consistently, CDKL3 knockdown induces cell apoptosis *in vitro* but suppresses tumor growth *in vivo*. Furthermore, CDKL3 knockdown increases p53 expression and reduces cell viability, and these effects are significantly weakened by the p53 inhibitor, PFT- α . In conclusion, the current study highlights that CDKL3 promotes TNBC progressions via regulating the p53 signaling pathway, suggesting that CDKL3 is a novel therapeutic target for TNBC treatment.

Key words: triple-negative breast cancer, cyclin-dependent kinase like 3, apoptosis, migration, p53 signaling pathway

Breast cancer (BC) is the most frequently diagnosed cancer and the leading cause of cancer death in women [1]. The incidence of this lethal disease with almost 1,700,000 new cases every year. Nowadays, available treatments for patients with BC include surgery, chemotherapy, radiation therapy, targeted therapy, and hormone therapy [2, 3]. Unfortunately, despite important advances in BC research, about 15–25% of triple-negative breast cancer (TNBC) patients present poor outcomes due to the unavailable targeted treatment, suggesting TNBC is still a major health problem [4]. TNBC, characterized by the absence of estrogen, progesterone, and human epidermal growth factor 2 receptors, is an aggressive subtype that frequently develops a resistance to chemotherapy and presents a particularly challenging therapeutic target [5]. Nowadays, therapies directed to specific molecular targets have rarely shown to be clinically meaningful to improve disease outcomes of patients with TNBC, and chemotherapy remains the standard of care [6]. Survival of TNBC patients after metastatic relapse is shorter compared to other breast cancer subtypes, treatment options are few, and response rates are poor and lack durability [7]. Identifi-

cation of novel biomarkers that can help to guide treatment decisions in TNBC remains a clinically urgent need.

Cyclin-dependent kinase like 3 (CDKL3), also known as NKIAMRE, is a putative serine kinase that is homologous to MAPKs and CDKs, and participates in cell growth and/or cell differentiation [8, 9]. Although some researchers have revealed the important role of CDKL3 in cancers, such as esophageal squamous cell carcinoma and cholangiocarcinoma (CCA) [10, 11], there is still a lack of reliable evidence to support the action and mechanism of CDKL3 for TNBC progression.

In the present study, we aimed to explore the effects of CDKL3 in the progression of TNBC through a series of lab experiments, both *in vitro* and *in vivo*. We focused on exploring the underlying molecular mechanisms and revealed the vital functions of CDKL3 on TNBC. The present findings provide a base that CDKL3 is able to serve as a novel biomarker for studying TNBC prognosis and may develop a new candidate gene for TNBC targeted therapy. Results in our study may provide insight into how CDKL3 regulates the progression of TNBC both *in vitro* and *in vivo*.

Materials and methods

Cell culture. In this work, we used three TNBC cell lines MDA-MB-468, MDA-MB-231, BT549, and the normal breast epithelial cell line MCF10A, which were all obtained from the Chinese Academy of Sciences (Shanghai, China). All cells were cultured and maintained in DMEM (Corning, Manassas, VA) supplementing with 10% fetal bovine serum (FBS) (Gibco, Grand Island, NY), and then incubated under the conditions of 5% CO₂ at 37 °C.

RNA extraction and RT-PCR. Total RNA was extracted carrying out from tissues and cultured cells using TRIzol reagent (Pufei Biotech Co, Ltd, Shanghai, China). Total RNA was reverse-transcribed into cDNA using PrimeScriptTM RT reagent kit with gDNA Eraser (Takara, Dalian, China). The cDNA samples were used as templates with appropriate primer sets to perform RT-PCR using SYBR Premix Ex Taq II (Takara, Dalian, China) on a Light Cycler 480 II RT-PCR System (Roche, Basel, Switzerland). GAPDH was used to normalize the relative mRNA expression as an internal reference. The primers information was as shown as follows: CDKL3 (Forward): 5'-TATCTGGGCTTTGGGCTGTA-3';

CDKL3 (Reverse): 5'-TGGGGTGTGAACTTGAGGA-3'; p53 (Forward): 5'-TCTGACTGTACCACCATCCACTA-3'; p53 (Reverse): 5'-CAAACACGCACCTCAAAGC-3'; GAPDH (Forward): 5'-TGACTTCAACAGCGACACCA-3'; GAPDH (Reverse): 5'-CACCTGTTGCTGTAGC-CAA-3'. The formula 2^{-ΔΔCT} method was used to process the relative gene expression data.

Immunohistochemical analysis. The clinical tissue microarray (TMA) was obtained from Shanghai Outdo Biotech Co., Ltd. TNBC tissues samples of TMA were obtained from the Changzhou Tumor Hospital Affiliated to Soochow University and Shanghai Shuguang Hospital Affiliated to Shanghai University of Traditional Chinese Medicine. No patients received chemotherapy or radiotherapy before surgery and all samples were followed up regularly for up to 5.6–10 years. These tissue samples contained 137 TNBC tumor tissues and 12 normal esophageal tissues and included 125 complete patient clinical information. The basic clinicopathological characteristics of 125 patients are summarized in Table 1. Briefly, sections (4 μm) were deparaffinized and then treated using 3% hydrogen peroxide for 10 min for quenching the endogenous peroxides activity. Sections were submerged into citric acid (pH 6.0) for antigenic retrieval. The slides were treated with 3% H₂O₂ and were then incubated with the primary antibodies (diluted at 1:100), including CDKL3 (bs-5747R, Bioss) and Ki-67 (ab15580, Abcam) at 4 °C overnight. Unrelated rabbit IgG secondary antibodies served as a negative control for primary antibodies and the slides were visualized using DAB. Each pathological section was evaluated by three independent pathologists who did not know the characteristics of all cases. A positive signal for CDKL3 was observed as dark brown/yellow brown coloring. The proportion of tumor cells was scored as follows [12]: 0, no tumor cells stained positive; 1, <25% of tumor cells stained positive; 2, 25–50% of tumor cells stained positive; 3, 50–75% of tumor cells stained positive; and 4, ≥75% of tumor cells stained positive. And the grade of staining intensity (SI) was classified as: 0, no cells stained positive; 1, weak stained positive, light yellow; 2, moderate stained positive, yellow brown; and 3, strong stained positive, dark brown. The patients were divided into two groups by median baseline CDKL3 expression.

Lentivirus packaging and infection. All plasmids used in our study were synthesized by GeneChem. The information of sequences was listed as follows: shCDKL3-1: 5'-GAGGAGATATCTCAGAACCAA-3'; shCDKL3-2: 5'-ACTAACTGTAATGGCTTGAAA-3'; shCDKL3-3: 5'-CACACAGTATTATGATGAGTTA-3'.

The scrambled control shRNA was used as a negative control. BT549 and MDA-MB-231 cells were selected and infected with lentiviral vectors using ENLS and Polybrene with a multiplicity of infection at 10 for overnight culture, followed by a changing of complete growth medium the next day. After 72 h, the infection efficiency of over 90% was evaluated using a fluorescence microscope (Olympus).

Table 1. Correlation between CDKL3 expression and clinical characteristics.

Variable	CDKL3 expression		p-value
	low	high	
All patients	64	61	
Age (years)			0.247
≤57	36 (56%)	28 (46%)	
>57	28 (44%)	33 (54%)	
Grade			0.009**
I/II	41 (64%)	25 (41%)	
III	23 (36%)	36 (59%)	
AJCC stage			0.709
1	13 (20%)	9 (15%)	
2	35 (55%)	35 (57%)	
3	16 (25%)	17 (28%)	
T stage			0.117
1	22 (34.4%)	12 (19.7%)	
2	36 (56.3%)	43 (70.5%)	
3	4 (6.3%)	6 (9.8%)	
4	2 (3.0%)	0 (0%)	
N stage			0.304
0	34 (53.1%)	29 (47.5%)	
1	17 (26.6%)	18 (29.5%)	
2	10 (15.6%)	6 (9.8%)	
3	3 (4.7%)	8 (13.1%)	
Tumor size			0.414
≤3 cm	33 (51.6%)	27 (44%)	
>3 cm	31 (48.4%)	34 (56%)	
Lymph node positive			0.532
=0	34 (53.1%)	29 (47.5%)	
>0	30 (46.9%)	32 (52.5%)	

Cell proliferation assay. The effect of CDKL3 on cell proliferation was measured by the CCK-8 assay. A total of 2×10^3 cells/well were seeded in a 96-well plate and incubated at 37 °C in a 5% CO₂ incubator. After culturing for 24, 48, 72, 96, 120 h, 10 µl/well of WST-8 working solution was added to each well. Next, the incubation for another 3 h at 37 °C away from light was performed. Finally, the absorbance at 450 nm was measured by a microplate reader. All experiments were performed in triplicate.

Cell apoptosis and cycle assays. The impact of CDKL3 on cell apoptosis and cell cycle distribution was detected using flow cytometry (FCM, Becton Dickinson, San Jose, CA, USA) with Annexin V-APC staining. Each experiment was performed in triplicate. Briefly, after 96 h of lentiviral infection, cells were washed twice with ice-cold binding buffer, centrifuged at 395×g for 3 min, and stained with 5 µl of Annexin V-APC reagent (eBioscience) for 15 min at room temperature in dark. Cell apoptosis was then analyzed by FCM. After infection for 96 h, cells were collected and flushed twice with ice-cold PBS on 4 °C. Then, 70% ice-cold ethanol was added for overnight incubation. The next day, cells were washed twice with PBS, adjusted to a concentration of 1×10^6 cells/well, and then stained with 500 µl propidium iodide (PI) in dark at room temperature for 30 min. Cell cycle distribution of G0/G1, S, and G2 was analyzed by FCM.

Transwell assay. Transwell chambers (Corning Inc., Corning, NY) were used to examine the impact of CDKL3 on the migration capacity of TNBC cells. Briefly, 6×10^4 cells in 100 µl serum-free DMEM medium were seeded into each upper chamber of 24-well Transwell, and 600 µl DMEM with 30% FBS was added into the lower chamber. After incubated 24 h for BT549 or 16 h for MDA-MB-231 in a 37 °C, 5% CO₂ incubator, the non-migrated cells in the upper chamber were gently removed with cotton swabs and the migratory cells were fixed with ethyl alcohol and then stained with 0.1% crystal violet (Yuanye Biotechnology Co. Ltd., Shanghai, China) for 5 min at room temperature. The migratory cells were counted under an inverted microscope, photographed, and then analyzed.

Western blotting assay. Cultured cells and tumors samples were lysed using passive lysis buffer (Roche). Total protein was determined using the BCA protein assay kit (Pierce), and the protein sample was separated by 12% SDS-PAGE, and electroblotted onto the polyvinylidene fluoride membranes. After blocking with TBST buffer containing 5% BSA and 0.02% sodium aside for 1 h, followed the incubation with 1:1000 diluted rabbit primary antibodies, including CDKL3 (Bioss), p53 (Abcam), and GAPDH (Bioworld), at 4 °C overnight. After being washed twice with TBST, the membranes were incubated with the secondary antibody horseradish peroxidase-conjugated goat anti-rabbit IgG (1:1000 diluted, Beyotime) for another 2 h. Target proteins were examined using the Pierce™ Fast Western Blot Kit (No. 35050, chemiluminescent substrate) (Thermo Fisher Scien-

tific) and images were photographed using AI600 (GE). GAPDH was used as a loading control.

Cell growth and tumor size in athymic nude mice determination. MDA-MB-231 cells transfected with shCtrl or shCDKL3-1 were washed and then resuspended in saline. Using trypan blue staining, cell number and cell viability was determined. 4-weeks old female athymic nude mice (Shanghai SLAC Laboratory Animal Co. Ltd.) were randomly divided into two groups (3 mice/each group) followed by the subcutaneous injection with 200 µl saline or MDA-MB-231 cells (1×10^7 cells/injection site). The mice were observed every day and data were measured twice a week after 27 days of injection. Tumor photographing and tumor weighting of tumor-bearing mice was performed immediately after euthanizing using CO₂ with control ventilation flow rate at 50% of sealed container ventilation flow rate for 5 min in a sealed container on day 58 post-inoculation. Tumor volume was calculated following: $\frac{1}{2} (\text{Length} \times \text{Width}^2)$. All animal experiments in our study were consistent with the ethical guidelines of the Helsinki Declaration and approved by the Ethics Committee of Changzhou Tumor Hospital Affiliated to Soochow University (approval NO: IACUC-2020-04-A).

Protein chip assay. Following the manufacturer's instructions, the apoptosis related signaling pathways underlying CDKL3 in MDA-MB-231 cells were identified using a Human Apoptosis Antibody Array Kit (Abcam, Cambridge, MA) after cell collection and lysis.

Promoter activity assay. MDA-MB-231 cells were transduced for 4–6 h with lentivirus encoding shCDKL3 or control shRNA. Then, the cells were transfected for 4–6 h with a plasmid expressing luciferase reporter under the control of a p53-driven promoter. Quantitation of luciferase activity allowed the assessment of promoter activity. Briefly, after 48 h transfection, cells were washed with PBS twice and harvested with passive lysis buffer from the dual-luciferase reporter assay system (Promega). Cells were lysed and centrifuged, and the cell supernatant was collected for detection. Aliquots of supernatant (40 µl) were added into 96-well plates, followed adding of 20 µl luciferase assay reagent (Promega) at room temperature. Luciferase activity was measured immediately using a luminometer (Orion II Microplate Luminometer, Berthold Detection Systems). Data were normalized to the results obtained for the internal control *Renilla* luciferase.

Statistical analysis. Prism8 (GraphPad) was used for statistical analysis of all collected data. Survival of 125 TNBC patients was performed using Kaplan-Meier analysis. The time from the date of diagnosis to the date of the last follow-up or death from any cause was defined as the overall survival. The clinical differences between patients with high or low expression of CDKL3 were analyzed using the Chi-square test. The difference was assessed using the Student's t-test between two groups. p values were a two-tailed test, and the level of significance was set at $p < 0.05$.

Results

CDKL3 is overexpressed in breast cancer tissues and is associated with a poor prognosis. To understand the functions of CDKL3 in TNBC, IHC was conducted to detect the CDKL3 expression in non-tumor tissues (n=12) and tumor tissues (n=137), and a higher expression level of CDKL3 was observed in TNBC tissues than those in non-tumor tissues (Figure 1A). Besides, CDKL3 was obviously higher in patients with higher histological grade (Figure 1B) and their corresponding statistical quantitative results are presented in Supplementary Figure S1A. Furthermore, a total of 125 patients with TNBC were divided into a high CDKL3-expression group and a low CDKL3-expression group with the median protein expression level as the cutoff value. Kaplan-Meier analysis indicated that a distinct longer overall survival was observed in the patients with a low expression of CDKL3, but patients with a high expression of CDKL3 possessed shorter overall survival (Figure 1C). In addition, the correlation between CDKL3 expression and clinical characteristics had been presented in Table 1, which revealed that high expressions of CDKL3 were mainly correlated with high tumor grade (p=0.009). The results of the RT-PCR assay revealed that CDKL3 expression was significantly higher in three TNBC cell lines (MDA-MB-468, MDA-MB-231, and BT549) than that in the human normal epithelial cell line, MCF-10A (Figure 1D). Moreover, bioinformatic analyses of the GEPIA2 databases (<http://gepia2.cancer-pku.cn/>) [13] indicated that a high CDKL3 expression closely correlated with low overall survival for breast invasive carcinoma (BRCA), liver hepatocellular carcinoma (LIHC), and stomach adenocarcinoma (STAD) in the GEPIA2 data set (Figure 1E). In conclusion, the present study demonstrated that CDKL3 is distinctly upregulated in TNBC tissues and cells, and associates with a poor prognosis, suggesting that CDKL3 may have a potential effect on the development and prognosis for TNBC.

CDKL3 promotes the proliferation and migration of TNBC cells *in vitro*. To determine the functional roles of CDKL3 in TNBC, CDKL3 was knocked down and overexpressed by using a lentiviral delivery system. Western blot analysis showed the successfully transfected shCDKL3-1~3 into MDA-MB-231 cells and shCDKL3-1 was the most effective interference target by the confirmation of the CCK-8 assay (Figures 2A, 2B). Hence, shCDKL3-1 was chosen for the follow-up experiments. To further disclose the function of CDKL3 in TNBC cells, we also checked the overexpression CDKL3 roles in MDA-MB-231 and BT549 cells, and the results of RT-PCR verified that both TNBC cells were successfully transfected with Ctrl, CDKL3, or shCDKL3 (Figure 2C). As shown in Figure 2D, the percentage of apoptotic cells was upregulated in the shCDKL3 group while reduced in the CDKL3 group (Supplementary Figure S1B) comparing to the Ctrl group, which indicated that the CDKL3 knockdown could increase apoptosis while the CDKL3 overexpression

could reduce the apoptosis of MDA-MB-231 and BT549 cells. In addition, the cell cycle blockade is one of the well-established antitumor mechanisms for many cancers. To understand the mechanism by which CDKL3 promotes BC cell proliferation, we thus analyzed the cell cycle of cells transfected with shCDKL3, shCtrl, or CDKL3. The population of the G1-phase and G2 cells were significantly increased in the shCDKL3 group but decreased in the CDKL3 group when compared with the Ctrl group, while cell populations in the S-phase were distinctly decreased in the shCDKL3 group (Figure 2E) but increased in the CDKL3 group (Supplementary Figure S1C). All these findings indicate that the CDKL3 knockdown could inhibit the proliferation of TNBC cells by blocking the cell cycle. Subsequently, CCK-8 assays and Transwell assays were performed to analyze cell viability and migration, which suggested that overexpression CDKL3 has exactly the opposite effect, compared with the shCDKL3 knockdown (Figures 2F–2I). Collectively, our results proved that CDKL3 could promote the proliferation and migration of TNBC cells *in vitro*.

Knockdown of CDKL3 inhibits tumor growth of TNBC cells *in vivo*. Xenograft assays were performed in nude mice and the development of solid tumors was monitored. A total of 1×10^7 shCDKL3-modified MDA-MB-231 cells and their control cells (shCtrl) were injected subcutaneously into the nude mice (n=3). The mice were weighed and tumor volumes were measured once a week from its formation until day 58. The xenografts produced from MDA-MB-231 cells with shCDKL3 were significantly slower than that of the shCtrl, and a smaller final tumor volume and weight (0.083 ± 0.126 g vs. 0.779 ± 0.347 g, *p<0.05) was observed after the knockdown of shCDKL3 (Figures 3A–3C). Furthermore, the expression of Ki-67 was detected by IHC, and tumor slides were stained by H&E. As shown in Figure 3D, Ki-67 expression in the shCtrl group was distinctly increased compared to the shCDKL3 group. Meanwhile, the CDKL3 expression of indicated tumors showed that CDKL3 was stable decrement during the growth of MDA-MB-231 in the mice (Figure 3E and Supplementary Figure S2A). Together, these findings demonstrated that CDKL3 contributed to promoting TNBC tumor growth *in vivo*.

CDKL3 inhibits the p53 signaling pathway in TNBC cells. A protein chip was performed to explore the possible function pathways using shCtrl or shCDKL3 MDA-MB-231 cells. The results proved that CDKL3 knockdown inhibited the protein expression level of Survivin and XIAP, while the protein expression level of Caspase3, BIM, Fas, IGFBP-5, p21, p27, and p53 were increased in MDA-MB-231 cells (Figures 4A, 4B, and Supplementary Figure S1D). Combined with the KEGG pathway analysis and protein network analysis using online tools, the p53 signaling pathway was identified as the most correlated signaling axis downstream with CDKL3 (Figure 4C). CDKL3 knockdown increased luciferase activity in the p53-driven luciferase reporter assay (Figure 4D). RT-PCR assays confirmed increased expression

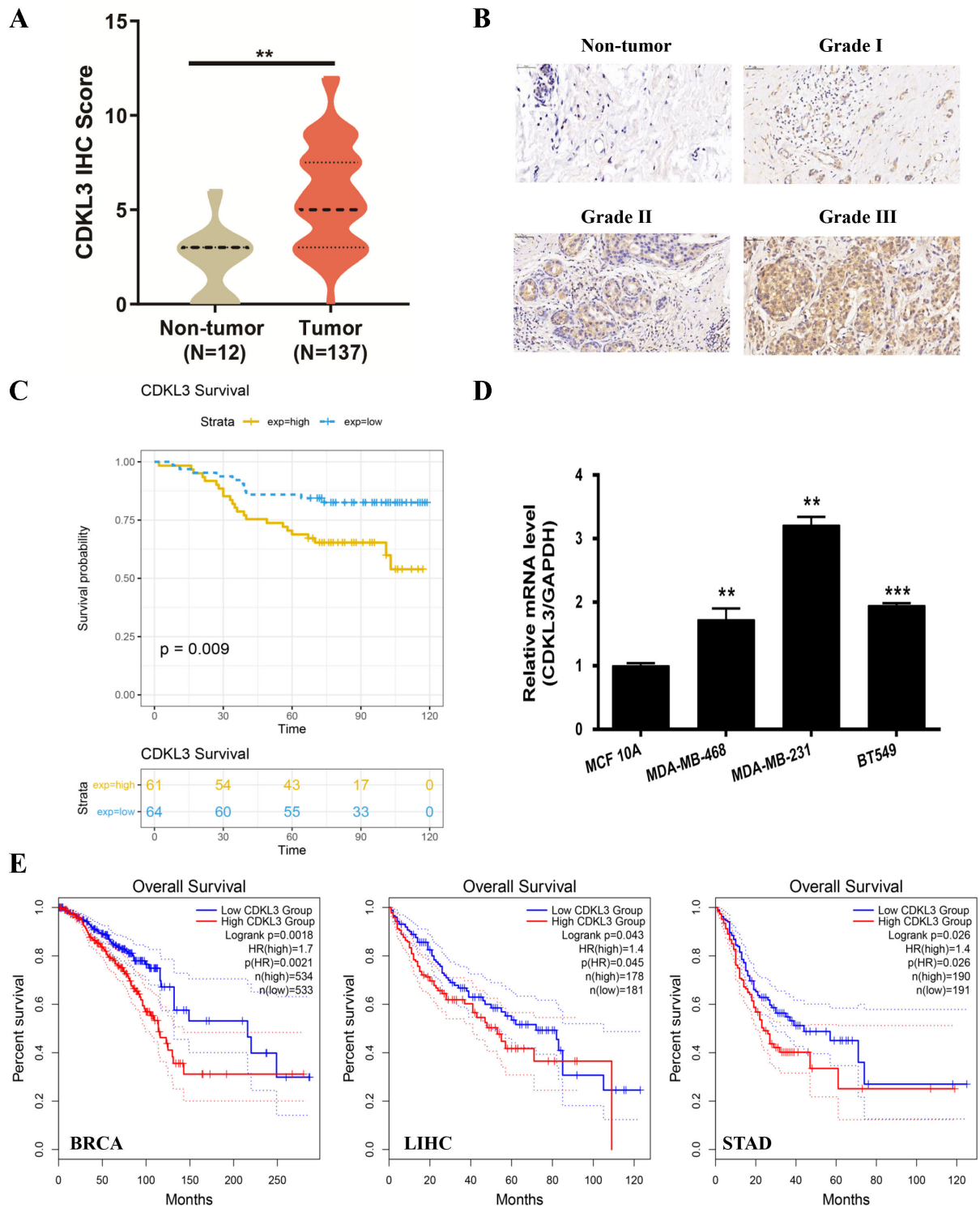


Figure 1. CDKL3 is highly expressed in breast cancer and is associated with a poor prognosis. **A)** The relative expression of CDKL3 protein in 137 BC tissues and 12 adjacent non-tumor tissues was checked by IHC. **B)** Representative images of CDKL3 expression in non-tumor tissues and different grade tumor tissues revealed in IHC analysis (bar: 50 μ m). **C)** The relationship between overall survival and CDKL3 expression was detected by Kaplan-Meier analysis. Median was defined as the best cut-off to divide the patients into the CDKL3 low group (n=64) and the CDKL3 high group (n=61). **D)** The relative expression of CDKL3 in three TNBC cell lines (MDA-MB-468, MDA-MB-231, and BT549) and the normal cell line MCF-10A was detected by RT-PCR. **E)** The relationship between overall survival and CDKL3 expression was obtained by GEPIA2. All experiments were performed in triplicate and results are presented as the mean \pm S.E.M, **p<0.01; ***p<0.001

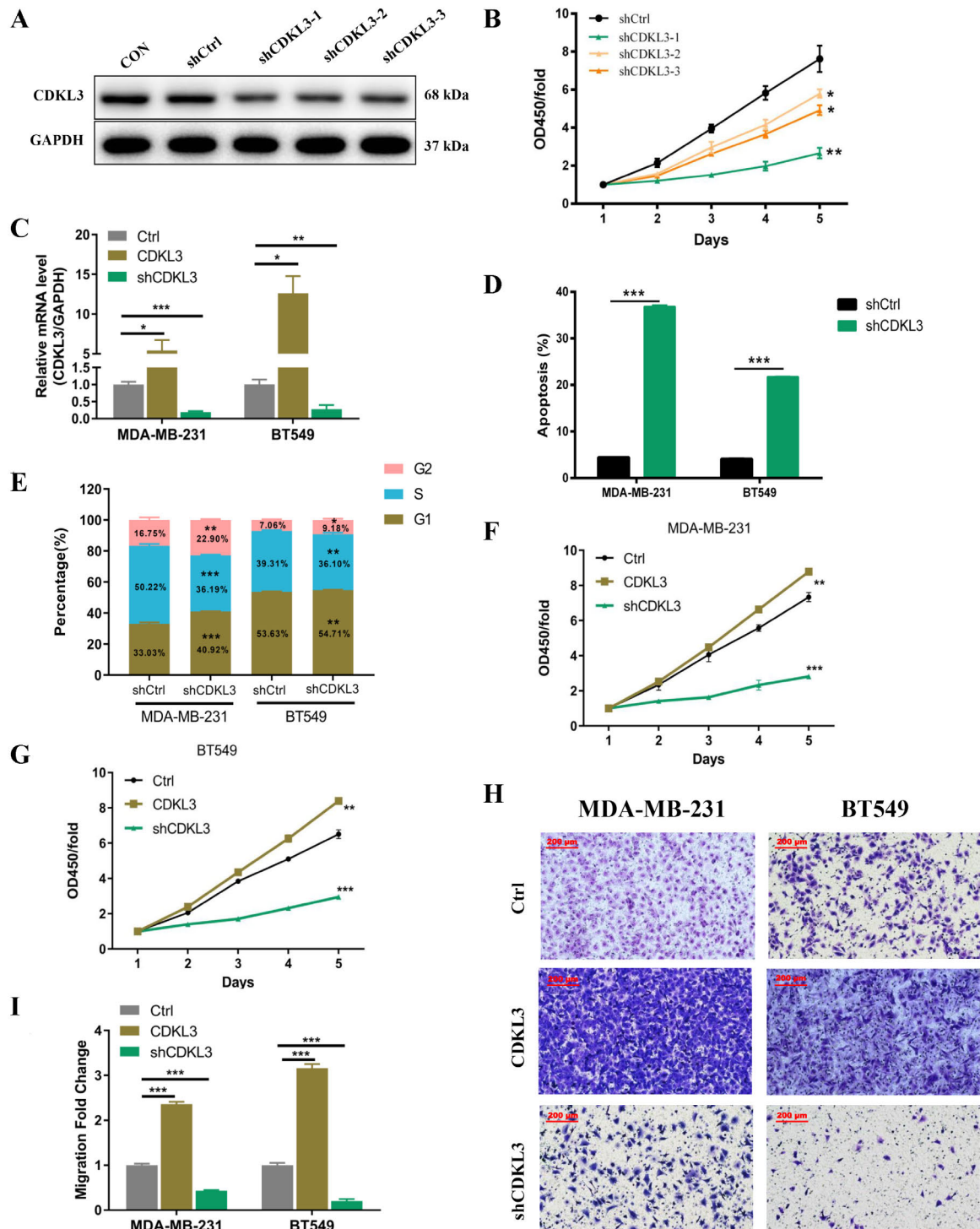


Figure 2. CDKL3 promotes the proliferation and migration of TNBC cells *in vitro*. **A**) Knockdown efficiency of CDKL3 in MDA-MB-231 cells was confirmed by WB. **B**) CCK-8 assays were performed to examine the viability of MDA-MB-231 cells transfected with shCDKL3 or shCtrl. **C**) The relative expression of CDKL3 in Control (Ctrl), CDKL3 knockdown (shCDKL3), and overexpression (CDKL3) cells was detected by RT-PCR. **D**) Flow cytometry was performed to analyze cell apoptosis of MDA-MB-231 and BT549 cells transfected with shCDKL3 or shCtrl. **E**) Flow cytometry was performed to analyze the cell cycle of MDA-MB-231 and BT549 cells transfected with shCDKL3 or shCtrl. **F**) CCK-8 assays were performed to examine the viability of MDA-MB-231 cells transfected with Ctrl, CDKL3, or shCDKL3. **G**) CCK-8 assays were performed to examine the viability of BT549 cells transfected with Ctrl, CDKL3, or shCDKL3. **H**) Transwell assays were performed to examine the migration of MDA-MB-231 and BT549 cells transfected with Ctrl, CDKL3, or shCDKL3 (scale bar: 200 μ m). **I**) The ability of cells to migrate is shown in the histograms. All experiments were performed in triplicate and results are presented as the mean \pm S.E.M, * p <0.05; ** p <0.01; *** p <0.001

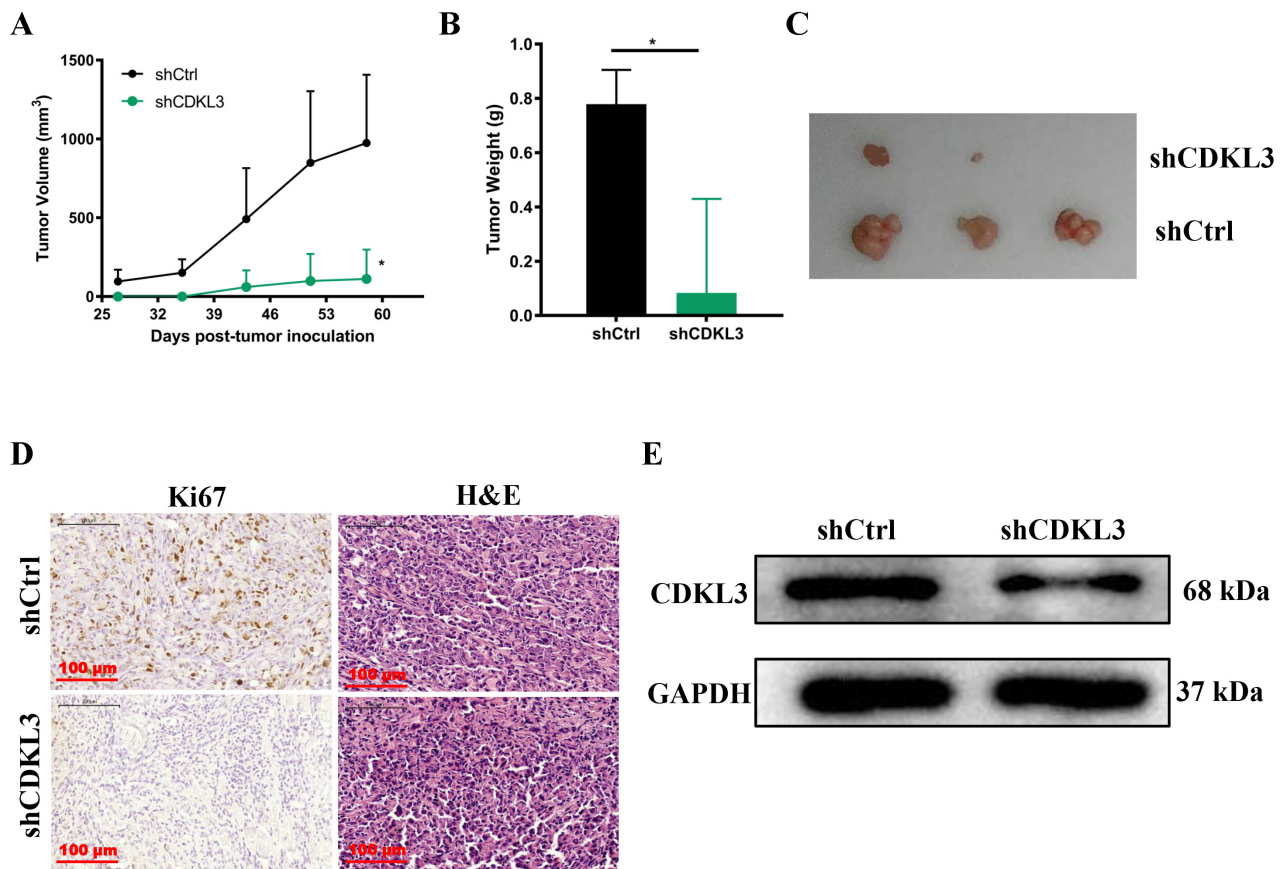


Figure 3. Downregulation of CDKL3 impairs tumor cells growth *in vivo*. **A**) Tumor volume was calculated every 8 days as the length \times width² \times 0.5. **B**) Tumor weight was measured after implantation after sacrificing mice. **C**) BALB/C nude mice (n=3) were simultaneously transplanted with MDA-MB-231 cells transfected with shCtrl or shCDKL3. **D**) Ki-67 (left) and H&E (right) staining were performed in xenograft (scale bar = 100 μ m). **E**) The expression of CDKL3 in MDA-MB-231 cells was confirmed by western blot. All experiments were performed in triplicate and results are presented as the mean \pm S.E.M, *p<0.01

of p53 at the mRNA level (Figure 4E). Western blot analysis verified that CDKL3 knockdown and CDKL3 overexpression increased and decreased the expression of p53 at the protein level, respectively (Figure 4F and Supplementary Figure S2B). As present in Figure 4G, the inhibitory effects of CDKL3 knockdown on cell viability of TNBC cells were attenuated when cells were treated with a p53 inhibitor Pifithrin- α (PFT- α , 10 μ M). In short, the knockdown of CDKL3 could induce apoptosis in MDA-MB-231 and BT549 cells by negatively regulating the p53 signaling pathway.

Discussion

In this study, combing *in vitro* and *in vivo* experiments, we uncover that CDKL3 is identified as an oncogene in TNBC. IHC data indicates that CDKL3 is upregulated in breast cancer tissues, and overexpression of CDKL3 is related to a poor prognosis of BC patients, suggesting a potential role of CDKL3 in the carcinogenesis of breast cancer. Consistently, bioinformatic analyses of public databases confirmed the

IHC results. Furthermore, a series of experiments *in vitro* and *in vivo* notarize the positive role of CDKL3 in promoting TNBC cell proliferation, cell cycle progression, apoptosis-resistance, migration, and tumor growth. Mechanistically, CDKL3 knockdown suppresses the progression of TNBC cells through activating the p53 signaling pathway. Consequently, this is the first report showing the roles and mechanism of CDKL3 as an oncogene in TNBC.

It is well known that TP53 encodes the transcription factor and tumor suppressor p53 [14]. It plays a central role in response to cellular stress signals, such as oncogenic stress or DNA damage [15]. If p53 is activated, transactivation of target genes by p53 leads to cell cycle arrest, DNA repair, or in cases of severe damage-apoptosis [14–16]. In addition, the p53 target genes are also involved in senescence, angiogenesis, and autophagy [17, 18]. In this present study, we confirm that CDKL3 serves as a novel oncogene in TNBC, inhibiting cell cycle arrest and cell apoptosis. To explore the further mechanisms, anti-apoptotic proteins (Survivin and XIAP) and pro-apoptotic proteins (Caspase3,

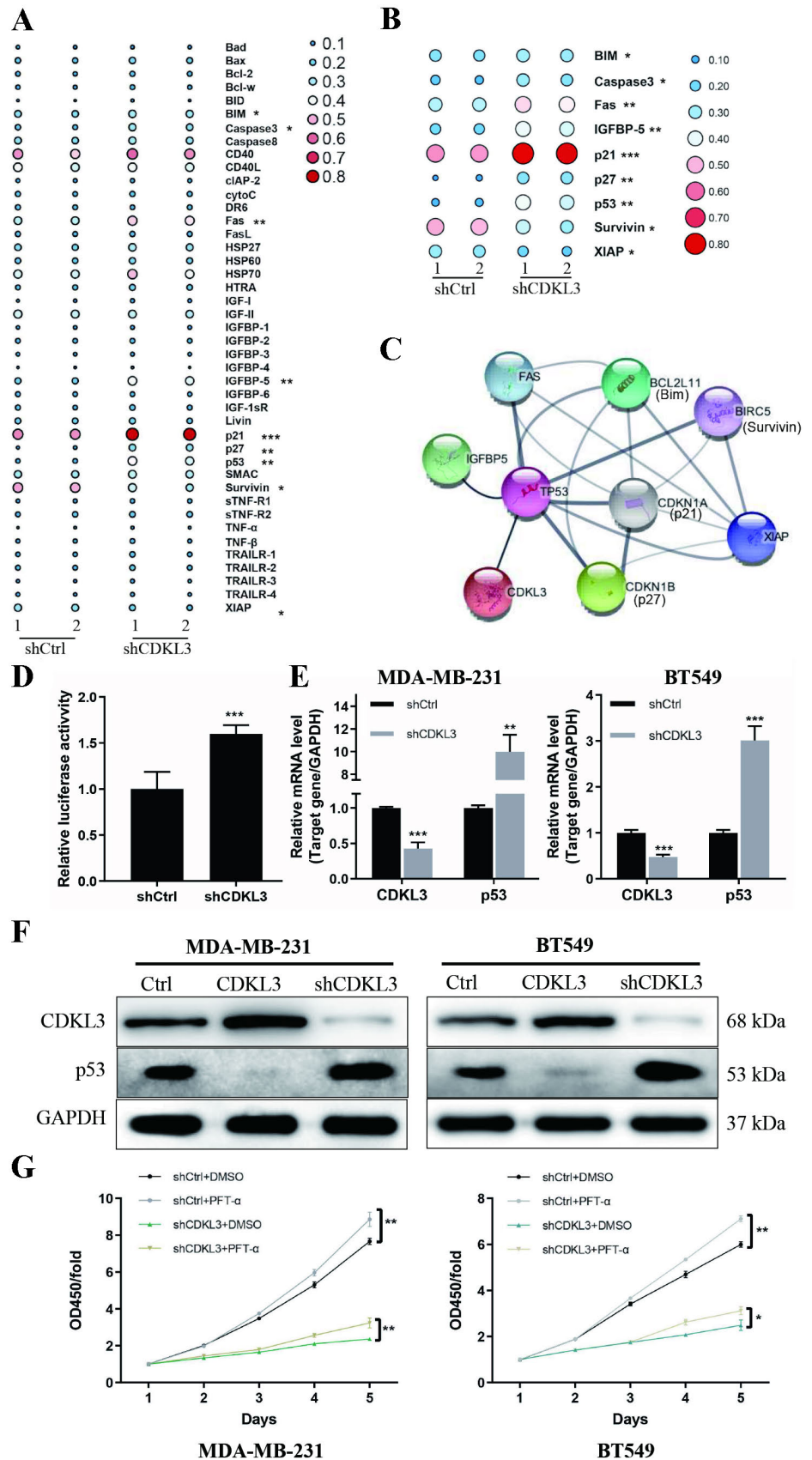


Figure 4. Exploration of the downstream molecular mechanism of CDKL3 in TNBC cells. A) Human apoptosis antibody array analysis was performed in MDA-MB-231 cells transfected with shCtrl or shCDKL3. B) The differential protein expression was performed in MDA-MB-231 cells transfected with shCtrl or shCDKL3. C) Differential Protein Network Analysis through the STRING database. D) A dual-luciferase assay was performed to determine the effect of CDKL3 knockdown on the transcriptional activity of TP53 in MDA-MB-231 cells. E) RT-PCR was performed to determine levels of p53mRNAs in both MDA-MB-231 and BT549 cells. F) The downstream proteins expression of p53 was observed by WB in MDA-MB-231 and BT549 cells transfected with Ctrl, shCDKL3, or CDKL3 OE. G) CCK-8 assays were performed to examine the viability of MDA-MB-231 and BT549 cells transfected with shCtrl or shCDKL3 and treated with or without PFT- α . All experiments were performed in triplicate and results are presented as the mean \pm S.E.M, * $p < 0.05$; ** $p < 0.01$; *** $p < 0.001$

BIM, Fas, IGFBP-5, p21, p27, and p53) were obtained by protein chip. Survivin and XIAP were members of the inhibitor of apoptosis (IAP) gene family, which encodes negative regulatory proteins that promote cell proliferation, prevent apoptotic cell death in the G2/M phase, and serve as an inhibitor of CASP3 and CASP7 [19–22]. Caspase3 is a cysteine-aspartic acid protease that plays a central role in the execution phase of cell apoptosis [23]. BIM is an apoptosis-inducing member of the Bcl-2 protein family and one of the potential mediators of p53-induced apoptosis [24, 25]. Fas is another potential mediator of p53-induced apoptosis, which belongs to the classic ‘death-signal’ receptors [26]. IGFBP5 has been demonstrated as a tumor suppressor, which induces apoptosis and cell cycle arrest in breast cancer cells [27, 28]. The p53 protein directly stimulates the expression of p21, an inhibitor of cyclin-dependent kinases (CDKs) that inhibits both the G1-to-S and G2-to-mitosis transitions [29]. The p53/p21 axis plays an important role in cell cycle inhibition and tumor suppression [30–32]. p21/p27 are cell cycle inhibitors that mediate CDK inhibition [33]. Together, the existing evidence supports the p53 signaling pathway as a tumor promotional mechanism in TNBC and p53 plays a central role in response to oncogenic stress from CDKL3. The data presented herein show that CDKL3 regulated p53 activity and its expression in TNBC cells. In addition, the inhibitory effects of CDKL3 were attenuated when cells were treated with the p53 inhibitor PFT- α . We thus proved that the CDKL3 knockdown inhibits TNBC by regulating the p53 signaling pathway.

Although the data in this study have demonstrated that CDKL3 is a definite oncogene for TNBC, more data are needed to validate it repeatedly. For instance, how is the biological change of CDKL3-overexpressing cells *in vivo*? Further study about the xenograft in nude mice and protein chip is needed as data shown here are from *in vitro* cell models.

In conclusion, our findings indicated that CDKL3 acts as an oncogene in TNBC, and the p53 signaling pathway is the main downstream effector underlying CDKL3 in TNBC. These findings reveal that CDKL3 is an ideal therapeutic target for TNBC treatment.

Supplementary information is available in the online version of the paper.

Acknowledgments: This work was supported by the Putuo Hospital Affiliated to Shanghai University of Traditional Chinese Medicine (2017315A).

References

- [1] BRAY F, FERLAY J, SOERJOMATARAM I, SIEGEL RL, TORRE LA et al. Global cancer statistics 2018: GLOBOCAN estimates of incidence and mortality worldwide for 36 cancers in 185 countries. *CA Cancer J Clin* 2018; 68: 394–424. <https://doi.org/10.3322/caac.21492>
- [2] DHANKHAR R, VYAS SP, JAIN AK, ARORA S, RATH G et al. Advances in novel drug delivery strategies for breast cancer therapy. *Artif Cells Blood Substit Immobil Biotechnol* 2010; 38: 230–249. <https://doi.org/10.3109/10731199.2010.494578>
- [3] BIANCHINI G, BALKO JM, MAYER IA, SANDERS ME, GIANNI L. Triple-negative breast cancer: challenges and opportunities of a heterogeneous disease. *Nat Rev Clin Oncol* 2016; 13: 674–690. <https://doi.org/10.1038/nrclinonc.2016.66>
- [4] DING L, CAO J, LIN W, CHEN H, XIONG X et al. The Roles of Cyclin-Dependent Kinases in Cell-Cycle Progression and Therapeutic Strategies in Human Breast Cancer. *Int J Mol Sci* 2020; 21: 1960. <https://doi.org/10.3390/ijms21061960>
- [5] MEDINA MA, OZA G, SHARMA A, ARRIAGA LG, HERNÁNDEZ JM et al. Triple-Negative Breast Cancer: A Review of Conventional and Advanced Therapeutic Strategies. *Int J Environ Res Public Health* 2020; 17: 2078. <https://doi.org/10.3390/ijerph17062078>
- [6] GARRIDO-CASTRO AC, LIN NU, POLYAK K. Insights into Molecular Classifications of Triple-Negative Breast Cancer: Improving Patient Selection for Treatment. *Cancer Discov* 2019; 9: 176–198. <https://doi.org/10.1158/2159-8290.Cd-18-1177>
- [7] KUMAR P, AGGARWAL R. An overview of triple-negative breast cancer. *Arch Gynecol Obstet* 2016; 293: 247–269. <https://doi.org/10.1007/s00404-015-3859-y>
- [8] MIDMER M, HAQ R, SQUIRE JA, ZANKE BW. Identification of NKIAMRE, the human homologue to the mitogen-activated protein kinase-/cyclin-dependent kinase-related protein kinase NKIATRE, and its loss in leukemic blasts with chromosome arm 5q deletion. *Cancer Res* 1999; 59: 4069–4074.
- [9] YEE KW, MOORE SJ, MIDMER M, ZANKE BW, TONG F et al. NKIAMRE, a novel conserved CDC2-related kinase with features of both mitogen-activated protein kinases and cyclin-dependent kinases. *Biochem Biophys Res Commun* 2003; 308: 784–792. [https://doi.org/10.1016/s0006-291x\(03\)01475-x](https://doi.org/10.1016/s0006-291x(03)01475-x)
- [10] YE W, ZHU J, HE D, YU D, YANG H et al. Increased CDKL3 expression predicts poor prognosis and enhances malignant phenotypes in esophageal squamous cell carcinoma. *J Cell Biochem* 2018. <https://doi.org/10.1002/jcb.27991>
- [11] ZHANG J, SU G, TANG Z, WANG L, FU W et al. Curcumin Exerts Anticancer Effect in Cholangiocarcinoma Cells via Down-Regulating CDKL3. *Front Physiol* 2018; 9: 234. <https://doi.org/10.3389/fphys.2018.00234>
- [12] JIANG S, MENG L, CHEN X, LIU H, ZHANG J et al. MEX3A promotes triple negative breast cancer proliferation and migration via the PI3K/AKT signaling pathway. *Exp Cell Res* 2020; 395: 112191. <https://doi.org/10.1016/j.yexcr.2020.112191>
- [13] TANG Z, KANG B, LI C, CHEN T, ZHANG Z. GEPIA2: an enhanced web server for large-scale expression profiling and interactive analysis. *Nucleic Acids Res* 2019; 47: W556–W560. <https://doi.org/10.1093/nar/gkz430>
- [14] VOGELSTEIN B, LANE D, LEVINE AJ. Surfing the p53 network. *Nature* 2000; 408: 307–310. <https://doi.org/10.1038/35042675>

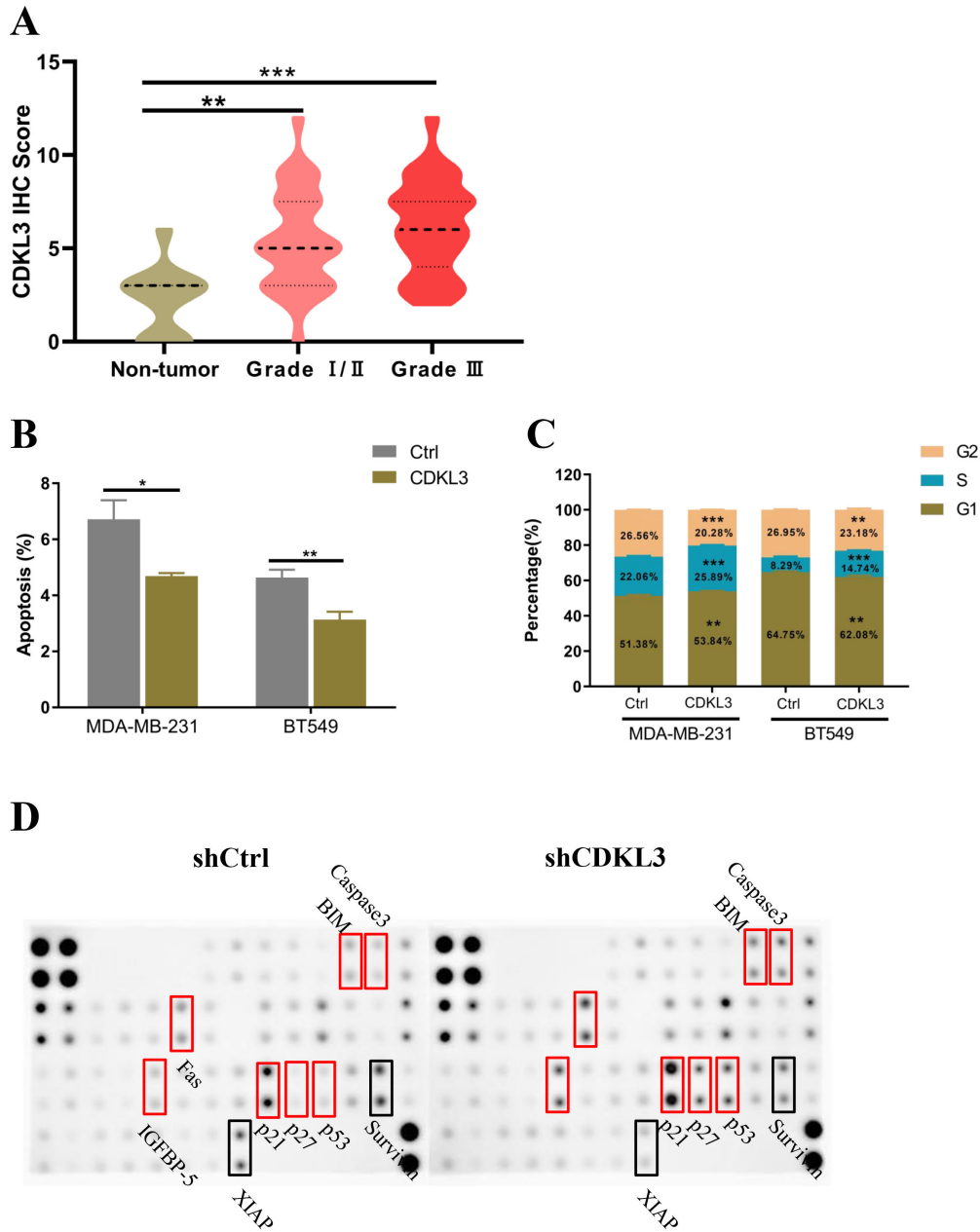
- [15] LANE D, LEVINE A. p53 Research: the past thirty years and the next thirty years. *Cold Spring Harb Perspect Biol* 2010; 2: a000893. <https://doi.org/10.1101/cshperspect.a000893>
- [16] JOERGER AC, FERSHT AR. The p53 Pathway: Origins, Inactivation in Cancer, and Emerging Therapeutic Approaches. *Annu Rev Biochem* 2016; 85: 375–404. <https://doi.org/10.1146/annurev-biochem-060815-014710>
- [17] VOUSDEN KH, PRIVES C. Blinded by the Light: The Growing Complexity of p53. *Cell* 2009; 137: 413–431. <https://doi.org/10.1016/j.cell.2009.04.037>
- [18] BIEGING KT, MELLO SS, ATTARDI LD. Unravelling mechanisms of p53-mediated tumour suppression. *Nat Rev Cancer* 2014; 14: 359–370. <https://doi.org/10.1038/nrc3711>
- [19] ELMALLAH MIY, COGO S, CONSTANTINESCU AA, ELIFIO-ESPOSITO S, ABDELFATTAH MS et al. Marine Actinomycetes-Derived Secondary Metabolites Overcome TRAIL-Resistance via the Intrinsic Pathway through Down-regulation of Survivin and XIAP. *Cells* 2020; 9: 1760. <https://doi.org/10.3390/cells9081760>
- [20] LI F, AMBROSINI G, CHU EY, PLESCIA J, TOGNIN S et al. Control of apoptosis and mitotic spindle checkpoint by survivin. *Nature* 1998; 396: 580–584. <https://doi.org/10.1038/25141>
- [21] PAVLYUKOV MS, ANTIPOVA NV, BALASHOVA MV, VINOGRADOVA TV, KOPANTZEV EP et al. Survivin monomer plays an essential role in apoptosis regulation. *J Biol Chem* 2011; 286: 23296–23307. <https://doi.org/10.1074/jbc.M111.237586>
- [22] KAMRAN M, LONG ZJ, XU D, LV SS, LIU B et al. Aurora kinase A regulates Survivin stability through targeting FBXL7 in gastric cancer drug resistance and prognosis. *Oncogenesis* 2017; 6: e298. <https://doi.org/10.1038/oncsis.2016.80>
- [23] ZHENG T, CHEN K, ZHANG X, FENG H, SHI Y et al. Knockdown of TXNDC9 induces apoptosis and autophagy in glioma and mediates cell differentiation by p53 activation. *Aging (Albany NY)* 2020; 12: 18649–18659. <https://doi.org/10.18632/aging.103915>
- [24] EL-DEIRY WS. Regulation of p53 downstream genes. *Semin Cancer Biol* 1998; 8: 345–357. <https://doi.org/10.1006/scbi.1998.0097>
- [25] GOTTLIEB TM, OREN M. p53 and apoptosis. *Semin Cancer Biol* 1998; 8: 359–368. <https://doi.org/10.1006/scbi.1998.0098>
- [26] KABIR SR, ASADUZZAMAN A, AMIN R, HAQUE AT, GHOSE R et al. Zizyphus mauritiana Fruit Extract-Mediated Synthesized Silver/Silver Chloride Nanoparticles Retain Antimicrobial Activity and Induce Apoptosis in MCF-7 Cells through the Fas Pathway. *ACS Omega* 2020; 5: 20599–20608. <https://doi.org/10.1021/acsomega.0c02878>
- [27] BUTT AJ, DICKSON KA, MCDOUGALL F, BAXTER RC. Insulin-like growth factor-binding protein-5 inhibits the growth of human breast cancer cells in vitro and in vivo. *J Biol Chem* 2003; 278: 29676–29685. <https://doi.org/10.1074/jbc.M301965200>
- [28] ZHANG L, LI W, CAO L, XU J, QIAN Y et al. PKNOX2 suppresses gastric cancer through the transcriptional activation of IGFBP5 and p53. *Oncogene* 2019; 38: 4590–4604. <https://doi.org/10.1038/s41388-019-0743-4>
- [29] EL-DEIRY WS. p21(WAF1) Mediates Cell-Cycle Inhibition, Relevant to Cancer Suppression and Therapy. *Cancer Res* 2016; 76: 5189–5191. <https://doi.org/10.1158/0008-5472.CAN-16-2055>
- [30] KONIARAS K, CUDDIHY AR, CHRISTOPOULOS H, HOGG A, O'CONNELL MJ. Inhibition of Chk1-dependent G2 DNA damage checkpoint radiosensitizes p53 mutant human cells. *Oncogene* 2001; 20: 7453–7463. [10.1038/sj.onc.1204942](https://doi.org/10.1038/sj.onc.1204942)
- [31] LEI K, LI W, HUANG C, LI Y, ALFASON L et al. Neurogenic differentiation factor 1 promotes colorectal cancer cell proliferation and tumorigenesis by suppressing the p53/p21 axis. *Cancer Sci* 2020; 111: 175–185. <https://doi.org/10.1111/cas.14233>
- [32] ZHU F, DAI SN, XU DL, HOU CQ, LIU TT et al. EFN2 facilitates cell proliferation, migration, and invasion in pancreatic ductal adenocarcinoma via the p53/p21 pathway and EMT. *Biomed Pharmacother* 2020; 125: 109972. <https://doi.org/10.1016/j.biopha.2020.109972>
- [33] CHEN Y, DU M, YUSUYING S, LIU W, TAN Y et al. Nedd8-activating enzyme inhibitor MLN4924 (Pevonedistat), inhibits miR-1303 to suppress human breast cancer cell proliferation via targeting p27(Kip1). *Exp Cell Res* 2020; 392: 112038. <https://doi.org/10.1016/j.yexcr.2020.112038>

https://doi.org/10.4149/neo_2021_210331N427

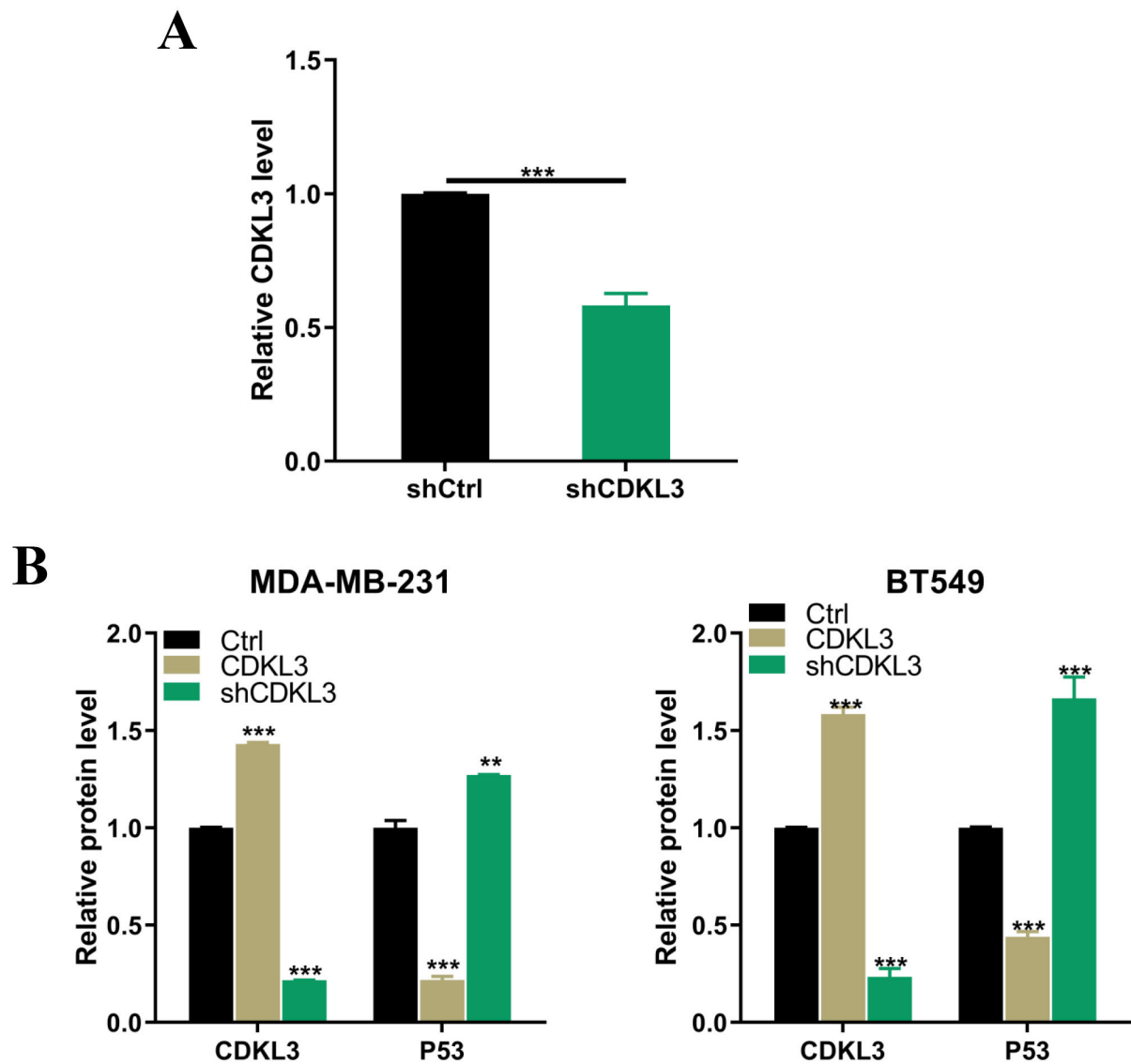
Cyclin-dependent kinase like 3 promotes triple-negative breast cancer progression via inhibiting the p53 signaling pathway

Dong-Xiang ZENG¹, Gui-Feng SHENG¹, Yong-Ping LIU¹, Ya-Ping ZHANG¹, Zheng QIAN², Zhe LI^{2*}, Yan-Zhi BI^{1*}

Supplementary Information



Supplementary Figure S1. CDKL3 regulates cell apoptosis and cell cycle of TNBC cells *in vitro*. A) The quantification of CDKL3 IHC score stratified by tumor grade (Grade I/II and Grade III) in Figure 1B. B) Flow cytometry was performed to analyze cell apoptosis of MDA-MB-231 and BT549 cells transfected with Ctrl or CDKL3. C) Flow cytometry was performed to analyze cell cycle of MDA-MB-231 and BT549 cells transfected with Ctrl or CDKL3. D) The original image of the human apoptosis antibody array analysis was performed in MDA-MB-231 cells transfected with shCtrl or shCDKL3. All experiments were performed in triplicate and results were presented as the mean±S.E.M, *p<0.05; **p<0.01; ***p<0.001



Supplementary Figure S2. Grayscale analysis of protein bands from western blot. A) The histogram shows the statistical results of gray level analysis of CDKL3 in Figure 3E. B) The histogram shows the statistical results of gray level analysis of CDKL3 and P53 in Figure 4F. All experiments were performed in triplicate and results were presented as the mean \pm S.E.M, ** p <0.01; *** p <0.001.